JOURNAL OF MATERIALS SCIENCE **34** (1999) 431–438

Application of instrumented falling dart impact to the mechanical characterization of thermoplastic foams

J. I. VELASCO*, A. B. MARTÍNEZ
Departament de Ciències dels Materials i Enginyeria Metal.lúrgica, Escola Tècnica Superior d'Enginyers Industrials de Barcelona (ETSEIB), Universitat Politècnica de Catalunya (UPC), Avda. Diagonal 647, 08028 Barcelona, Spain
E-mail: JVELASCO@CMEM.UPC.ES

D. ARENCÓN
Centre Català del Plàstic (CCP), Vapor Universitari de Terrassa. C/Colom 114, 08222 Terrassa, Spain

M. A. RODRÍGUEZ-PÉREZ, J. A. DE SAJA
Departamento de Física de la Materia Condensada, Cristalografía y Mineralogía, Universidad de Valladolid, Facultad de Ciencias. Prado de la Magdalena s/n, 47011 Valladolid, Spain

The applicability of instrumented falling weight impact techniques in characterizing mechanically thermoplastic foams at relatively high strain rates is presented in this paper. In order to try simulating impact loading of foams against sharp elements, an instrumented dart having a hemispherical headstock was employed in the tests. Failure strength and toughness values were obtained from high-energy impact experiments, and the elastic modulus could be measured from both flexed plate and indentation low-energy impact tests. The results indicate a dependence of the failure strength, toughness, and the elastic modulus on the foam density, the foaming process, and the chemical composition. This influence was found to be similar to that of pure nonfoamed materials and also to that observed from low-rate compression tests. The results also indicate that the indentation low-energy impact tests were more accurate in obtaining right values of the elastic modulus than the flexed plate low-energy impact tests usually used to characterize rigid plastics. The foam indentation observed with this test configuration contributes to obtaining erroneous values of the elastic modulus if only a simple flexural analysis of plates is applied.

1. Introduction

Traditionally, impact tests have been employed to measure the ability of a sample or a finished part to absorb a shock or impact. Falling weight impact tests stand out among the different types of impact tests because the simply supported or fixed (clamped) sample receives the collision of a mass falling from a determined height. These tests have the advantage of multiaxiality and the possibility of working with finished articles, if they are properly fixed.

The noninstrumented (analogic) impact tests give neither qualitative information about the energy required for the fracture initiation nor the information about the mechanical behavior of the material. These tests give only statistical plots as a relationship between the probability of failure or survival of the sample according to the strictness of the test [1].

Nevertheless, in instrumented impact tests, the recorded force that the striker supports during the test allows for the obtaining of information about the energy absorbed by the material until the failure. Carrying out low-energy tests (rebound), makes it possible to get information about its elastic properties. Therefore, using instrumented impact techniques, it is even possible to characterize the fracture behavior of plastics and composites by applying the linear-elastic fracture mechanics (LEFM) on SENB geometry [2, 3] to obtain fracture criteria such as the fracture energy (G_{IC}) and the fracture toughness (K_{IC}), which are independent of the geometry of the cracked body. However, this application is restricted to brittle materials.

The aim of this paper is to present a mechanical characterization of polyolefinic foams at relatively high strain rates by means of instrumented falling weight

* To whom correspondence should be addressed.

impact tests. These materials show the advantages of its thermoplastic character as well as of its closed-cell structure, such as easy recycling and good behavior as a thermal, acoustic, and moisture isolator, among other properties. Usually, the mechanical features of this kind of material have been determined by compression tests at low strain rates; nevertheless, this foam can be used for cushioning shock in packaging applications, which justifies its mechanical study at high strain rates. In this sense, Mills *et al.* [4] and Loveridge *et al.* [5] have applied falling weight impact techniques to characterize several thermoplastic foams, using a falling compression plate joint to an accelerometer. This test configuration does not take into account that the impact is often caused by a sharp element. The use of narrow hemispherical headstocks in instrumented falling weight impact tests permits the simulation of the collision between the foam and a sharp element at high speed, and therefore, measures the energy absorbed by the foam resulting from the total penetration of the striker, that is, an estimation of the foam toughness. Further, in carrying out low-energy impact experiments information has been obtained about the elastic modulus of the foams under study. Traditionally, the elastic modulus of rigid plastics has been obtained by rebound tests applying the elastic theory of flexed plates, but in the foamed materials, parasite strains, such as indentation, occur with this geometry test. In this work, the values of the elastic modulus of the foams obtained from pure indentation tests by rebound are compared.

2. Theoretical background

2.1. The static analysis

If the dynamic effects observed in the impact test are small, one can accept that the striker is always in contact with the sample during the test and, therefore, the phenomena can be considered as static and can be likewise analysed [6]. The equations of the static analysis for falling weight impact on flexed plates are the following:

$$a(t) = \frac{F(t) - P}{m} \tag{1}$$

$$v(t) = v_0 - \int_0^t \frac{F(t) - P}{m}\, dt \tag{2}$$

$$x(t) = \int_0^t v_0 - \int_0^t \left(\frac{F(t) - P}{m}\, dt \right) dt \tag{3}$$

$$U(t) = v_0 \int_0^t (F(t) - P)\, dt - \frac{1}{2m} \left(\int_0^t (F(t) - P)\, dt \right)^2 \tag{4}$$

In these equations F, x, v, a, and U represent the force, displacement, speed, acceleration, and energy at each instant, respectively. P is the weight and m is the effective falling mass. This static analysis is applicable when the velocity loss of the falling mass during the impact event is negligible.

2.2. The quasi-static model

The collision of a rigid striker with a homogeneous, linear-elastic material sample can be modelled considering the sample as a spring of rigidity, k. If the sample mass is negligible with regard to the striker one, the spring mass can be neglected, and hence, the equivalent mass of the system is that of the striker [7]. According the Newton's second law:

$$F = -kx = ma \tag{5}$$

$$ma + kx = 0 \tag{6}$$

The solution is of the type

$$x = A_1 \cos(\omega t) + A_2 \sin(\omega t) \tag{7}$$

Where ω is the angular frequency of the system

$$\omega = \sqrt{\frac{k}{m}} \tag{8}$$

When $t = 0$, $x = x_0$ and $v = v_0$, and then $A_1 = x_0$ and $A_2 = v_0/\omega$, the solution is:

$$x(t) = x_0 \cos(\omega t) + \frac{v_0}{\omega} \sin(\omega t) \tag{9}$$

In function of the phase angle (ψ):

$$x(t) = A \sin(\omega t + \psi) \tag{10}$$

where

$$A = \sqrt{A_1^2 + A_2^2} = \sqrt{x_0^2 + \left(\frac{v_0}{\omega} \right)^2} \tag{11}$$

and

$$\psi = \arctan \frac{A_1}{A_2} = \arctan \frac{x_0\, \omega}{v_0} \tag{12}$$

When the striker kicks the sample, $t = 0$, $x_0 = 0$, and $\psi = 0$. Also consider:

$$A = \frac{v_0}{\omega} \tag{13}$$

$$a = -v_0 \omega \sin(\omega t) \tag{14}$$

The force applied is as follows:

$$F(t) = -\sqrt{2U_0 k} \sin \sqrt{\frac{k}{m}} t = -F_{\max} \sin \frac{\pi t}{t_c} \tag{15}$$

where

$$F_{\max} = (2U_0 k)^{1/2} \tag{16}$$

$$t_c = \pi \sqrt{\frac{m}{k}} \tag{17}$$

$F_{\max}$ is the maximum force supported by the sample, and the contact time (t_c) is the time that the striker is

in contact with the sample. This model easily simulates the elastic behavior of the sample.

2.3. The indentation model

An indentation model has been collected by Greszczuk *et al.* [8], who describes the indentation phenomena of a hemispherical element on a material sample. It can be developed from the pressure distribution between the two elements. Denoting the mass and the velocity of the striker as m_1 and v_1, respectively, the target mass and its velocity as m_2 and v_2. The rates of change of velocity during the impact as the two bodies come in contact, are

$$\frac{dv_1}{dt} = -Fm_1, \qquad \frac{dv_2}{dt} = -Fm_2 \tag{18}$$

In the following, α denotes the distance from which the striker and the target approach one another because of local compression at the point of contact (penetration). The velocity of this approach is

$$\frac{d\alpha}{dt} = v_1 + v_2 \tag{19}$$

Results obtained by Rayleigh [9] showed that if the contact time between the striker and the target is very long in comparison with their natural periods, the vibrations of the system could be neglected. It can, therefore, be assumed from Hertz's law [10]:

$$F = n\alpha^{3/2} \tag{20}$$

This law was established for static conditions. The term n is defined as:

$$n = \frac{4\sqrt{R_1}}{3\pi(k_1 + k_2)} \tag{21}$$

Where R_1 is the radius of the spherical striker or indenter, and k_1 and k_2 are the rigidity of the striker and the target, respectively. Differentiating Equation 19, combining it with Equation 18, and the substitution of Equation 20 into resultant equation yields the following:

$$\frac{d^2\alpha}{dt^2} = nM\alpha^{3/2} \tag{22}$$

where

$$M = \frac{1}{m_1} + \frac{1}{m_2} \tag{23}$$

Proceeding now as in Timoshenko [11], if both sides of Equation 22 are multiplied by α, if and the resultant equation is integrated, the following results

$$\left(\alpha^2 - v_0^2\right) = -\frac{4}{5}Mn\alpha^{5/2} \tag{24}$$

where v_0 is the approach velocity of the two bodies at $t = 0$. The maximum penetration, α_1, occurs when the force is maximum ($F = F_{\max}$):

$$\alpha_1 = \left(\frac{5v_0^2}{4Mn}\right)^{2/5} \tag{25}$$

An alternate way of arriving at the relationship given by Equation 25 is to start the analysis with the energy balance of the system. Assuming that the target is semi-infinite and stationary, the energy balance becomes:

$$\frac{1}{2}m_1v_0 = \int_0^{\alpha_1} F\,d\alpha \tag{26}$$

Substitution of Equation 20 into Equation 26 followed by evaluation of the resulting integral gives

$$\frac{1}{2}m_1v_0^2 = \frac{2}{5}n\alpha_1^{5/2} \tag{27}$$

which is identical to the result given by Equation 25 when solved for α_1. It must be noted that in this case $M = 1/m_1$.

Substitution of Equation 25 into Equation 20 gives the following final relationship

$$F_{\max} = n^{2/5}\left(\frac{5v_0^2}{4M}\right)^{3/5} \tag{28}$$

In addition, Equation 24 can be rewritten as

$$dt = \frac{d\alpha}{\left(v_0^2 - \frac{4}{5}Mn\alpha^{5/2}\right)^{1/2}} \tag{29}$$

Integrating and solving yields:

$$t_c = 2.94\frac{\alpha_1}{v_0} = 2.94\left(\frac{5}{4Mnv_0^{1/2}}\right)^{2/5} \tag{30}$$

Equation 28 and Equation 30 show the maximum force and the contact time (t_c) dependence on n respectively, that is, on k_1 and k_2. The rigidity is related to the material elastic modulus (E) through

$$k = \frac{1 - \nu}{\pi E} \tag{31}$$

where ν represents the Poisson's coefficient of the material.

3. Materials

The name, chemical composition, density, and thickness of the industrial foamed materials under study are summarized in Table I. These foams are polyolefine-based compounds and have been kindly provided by ALVEO (Roermond, Holland).

Two groups of foams can be distinguished depending on their foaming process. The first group is ALVEOLIT ('T' samples), which are physically cross-linked foam sheets. In this foaming method, the sheet is slightly cross-linked by a high-energy electron beam before the

TABLE I Reference, chemical composition, density, and thickness of the foams

Reference	Chemical composition	Density (kg/m^3)	Thickness (mm)
NA 1106	LDPE	85	6.23
NA 2006	LDPE	48	6.23
NA 3308	LDPE	29	7.92
TA 1504	LDPE	62	4.02
NLB 1106	50%LDPE-50%LLDPE	89	5.83
NLB 1408	50%LDPE-50%LLDPE	67	7.81
NLB 2910	50%LDPE-50%LLDPE	33	10.00
TL 2005	50%LDPE-50%LLDPE	49	5.09
TL 3008	50% LDPE-50%LLDPE	31	8.43
NEE 1109	90%EVA (14%VA)-10%LDPE	86	8.71
NSR 2512	50%EPR-50%EVA	36	12.06
NT 0905	60%LDPE-40%HDPE	105	4.73
NT 2510	60%LDPE-40%HDPE	37	10.81

chemical blowing agent in the sheet is heat activated. Foaming is free, and foaming direction is vertical. This means that the foamable sheet passes from top to bottom through a hot oven, and the expanding sheet supports itself by gravity in the vertical direction. As a consequence of this treatment, the shape of the formed cells is slightly elongated in the vertical direction [12]. The second group, ALVEOLEN ('N' samples), are fabricated in a similar way, although the foaming process is carried out in a horizontal plane. Because of this configuration, the shape of the cells is almost spherical. After expansion both types of foams are passed through cooling rolls and wound up.

The foam samples were received as sheets of 250 mm × 400 mm having variable thickness, depending on the type of foam. From these sheets, circular plates of diameter 80 mm were cut off to use as test specimens.

4. Experimental procedure

4.1. Density measurement

Foam samples were conditioned at 24 °C and 50% relative humidity for 24 hours and subjected to density measurements in accordance with ASTM D1622.

4.2. Instrumented falling weight impact tests

Falling weight impact tests were carried out using a CEAST *DARTVIS* (Torino, Italy) instrumented impact equipment. The dart employed had a hemispherical headstock of diameter 12.7 mm, instrumented by extensometric gauges. In the test, the sample is supported on a rigid ring with inner and outer diameters of 60 and 80 mm, respectively.

Three types of tests were performed at room temperature. Firstly, high-energy or failure tests, employing a falling mass of 3743 g and a drop height of 990 mm, employing the sample plate clamped between two rigid rings of inner and outer diameter 60 and 80 mm, respectively. At these conditions the dart totally penetrated the foams, and both the dynamic effects and the percentage of energy lost by the striker were negligible. Then, the static analysis could be applied from the data recorded to obtain foam strength and foam toughness values. Secondly, two kinds of low-energy or rebound tests were carried out using a falling mass of 743 g. At least twelve tests, at different drop heights in the range 13–200 mm, were carried out per foam. On one hand, in the same way as in high-energy tests, clamped flexed plate geometry was imposed, and on the other hand, indentation tests were performed with the sample simply supported on a 10 mm thick steel plaque to avoid any flexion effects. In both cases, the rigidity (k), and therefore, the elastic modulus of the foams (E) could be measured from the recorded $F_{\max}$ and t_c values.

4.3. Scanning electron microscopy

Qualitative image analysis was used to assess type of cellular structure. For this purpose, cross-sectioned of extrudate were microtomed at a low temperature to provide a smooth surface which, after vacuum coating with gold, was examined by scanning electron microscopy (SEM) using a JEOL JSM 820.

5. Results and discussion

5.1. Failure behavior

In the high-energy impact tests, all of the samples were fully perforated by the dart, and the loss of velocity of the dart during the event was never higher than 5%; therefore, the static analysis could be applied to obtain values of energy. An example of the recorded force versus time curves is shown in Fig. 1, and the numerical results are collected in Table II. To get an estimation of the foam toughness, the values of energy were normalized by dividing them by the specimen volume.

The foam strength was taken as the maximum stress value ($\sigma_{\max}$) obtained from the equation for clamped flexed plates [13]:

$$\sigma_{\max} = \frac{F_{\max}}{h^2}(1+\nu)\left(0.485\log\frac{b}{h}+0.52\right) \quad (32)$$

TABLE II Values of the foam toughness and strength

Reference	Toughness (10^{-4} J/mm^3)	Strength (N/mm^2)
NLB 1106	1.765	9.241
NLB 1408	1.224	4.344
NLB 2910	0.622	1.669
TL 2005	0.806	5.582
TL 3008	0.520	1.986
NA 1106	1.132	6.673
NA 2006	0.636	3.968
NA 3308	0.201	1.288
TA 1504	0.783	8.803
NEE 1109	2.018	5.197
NSR 2512	0.677	1.107
NT 0905	1.166	12.868
NT 2510	0.412	1.383

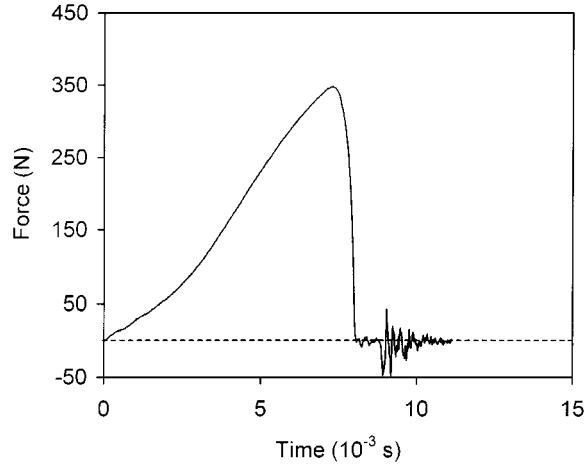

Figure 1 A typical curve obtained from failure tests (NEE 1109 foam).

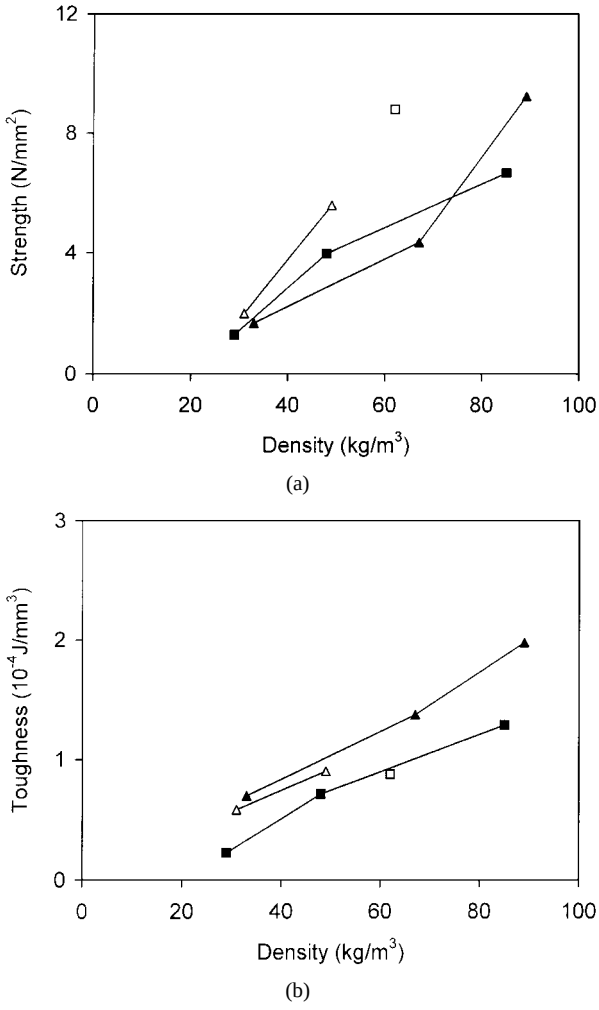

Figure 2 (a) Strength, and (b) toughness of ■ LDPE, ▲ 50%LDPE-50%LLDPE horizontal (N) foams. The hollow symbols correspond to vertical (T) foams with the same composition.

where ν is the Poisson's ratio, taken as 0.35, b the inner ring radius, and h the thickness of the sample.

As expected, in all the studied foams, both toughness and strength increased with regard to the foam density [14, 15], as shown in Fig. 2. The foaming direction (horizontal or vertical) seems not to affect to the foam toughness because this value depends mainly on the fraction of the sample able to release strain energy.

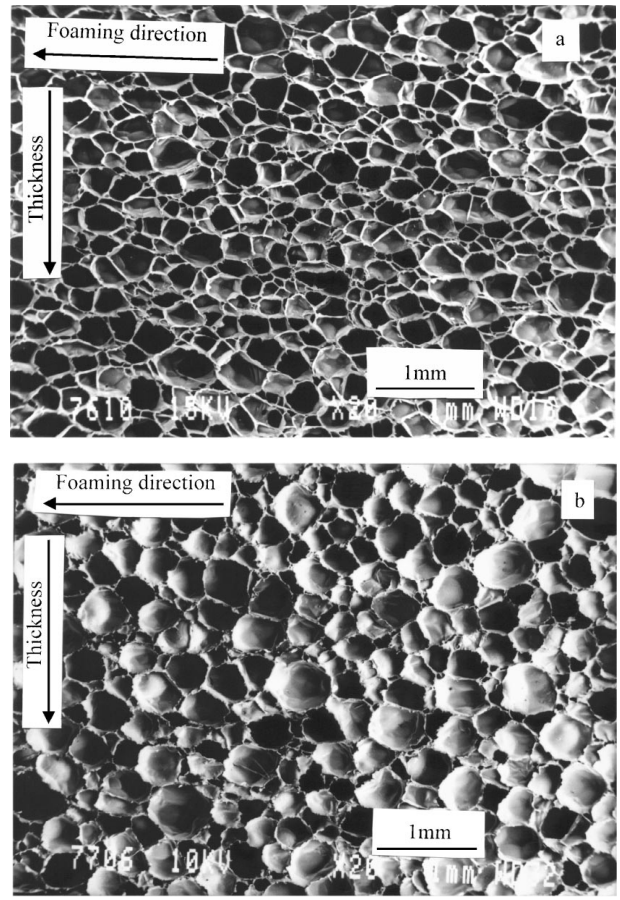

Figure 3 Micrographs by SEM of two typical samples. (a) TL 2005 foam and (b) NLB 1408 foam.

However, the values of strength obtained for vertical foams seem to be slightly higher than those corresponding to horizontal foams. This difference can be explained on the basis of the cell morphology that the foaming process provokes. In vertical foams, the cells are slightly elongated in parallel direction to the sample surface (Fig. 3a), that is, parallel to the maximum stress imposed on the sample during the test; whereas the horizontal foams have approximately spherical cells (Fig. 3b). Therefore, T samples have higher molecular orientation in the direction of the maximum stress applied, which results in higher strength values than N foams.

To analyze the influence of the foam composition, two groups of horizontal foams with different compositions can be distinguished in this paper. These distinctions can be made according to their similar density range (30–40 kg/m^3 and 90–100 kg/m^3). Their toughness and strength values are represented in Fig. 4. In the lower density group, small differences in the mechanical characteristics have been observed, especially noticeable is the constancy of the strength values. In this sense, the lower density, the smaller the contribution of the polymeric matrix to the sample strength and toughness. Therefore, smaller differences are due to the polymeric composition. Thus, to observe the effect of the composition, the group of foams with higher densities were focused upon. It must be noted that EVA-based foam showed the highest toughness and the lowest strength, because of its rubbery

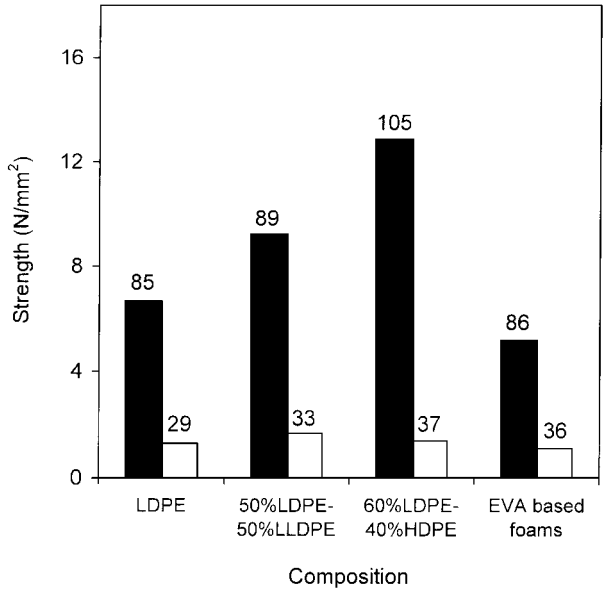

(a)

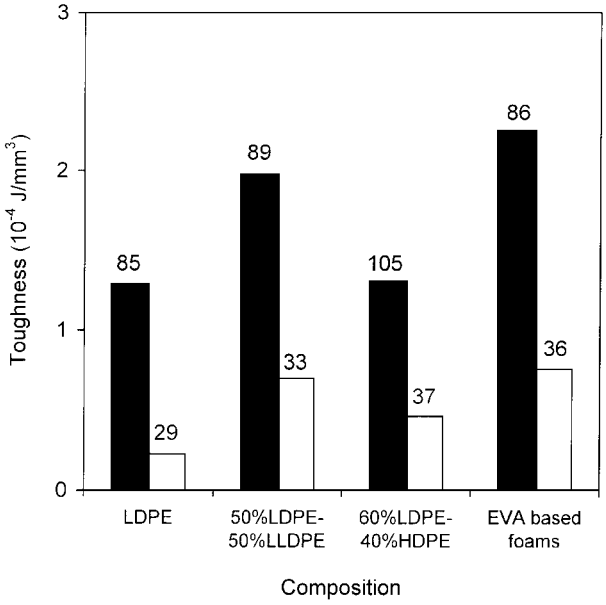

(b)

Figure 4 (a) Strength, and (b) toughness of the two groups of foams with similar density. Values above the bars indicate the foam density.

character, which allows it to be strained at low stress levels. The foam containing 60%HDPE showed higher strength and slightly lower toughness than the pure LDPE foam because of the more crystalline and rigid structure of the HDPE polymer, which is less branched than LDPE and so more packaged. Moreover, the foams containing 50%LLDPE showed both higher toughness and strength than the pure LDPE foams, which represent the best balance of properties of all the studied foams.

5.2. Elastic modulus from flexed plate geometry

From the $F_{\max}$ and t_c values obtained by rebound tests with flexed plate geometry, the value of the foam rigidity can be calculated in two ways (Equations 16 and 17). Examples of the recorded force/time curves are shown in Fig. 5. The rigidity of clamped flexed plates is related to the modulus of elasticity by the following expression [13]:

$$k = \frac{4\pi E h^3}{3b^2 (3 + \nu)(1 - \nu)} \tag{33}$$

Then, for each foam, two values of k, and therefore, two values of E ($E_{F\max}$ and E_{tc}) as the two respective mean values of all the rebound tests were obtained. These values are collected in Table III.

In general, the effect of the foam density and the foaming process on the E values (Fig. 6) is the same as the strength and toughness values obtained from high-energy experiments. Notice that the higher foam density, the higher modulus of elasticity, and that vertical T foams are more rigid than the corresponding horizontal N foams due to the elongated cells. As cited before, two groups of foams can be considered because of their similar density ranges for studying the effect of the chemical composition on the elastic modulus. Again, nonrepresentative differences in the E values of the lower density foams (Fig. 7) were found which must be due to experimental error. However, in the group of higher densities, the foam containing HDPE clearly shows the highest value of the elasticity modulus due

TABLE III Values of the elastic modulus obtained from flexed plate and indentation rebound tests

Foam sample	Flexed plates		Indentation
	$E_{F\max}$ (N/mm^2)	E_{tc} (N/mm^2)	E_{ind} (N/mm^2)
NLB 1106	8.615	7.026	2.356
NLB 1408	2.798	1.832	1.367
NLB 2910	1.118	0.542	0.706
TL 2005	10.596	3.449	0.791
TL 3008	2.335	0.673	0.583
NA 1106	5.968	4.346	2.020
NA 2006	5.533	2.105	0.892
NA 3008	2.422	1.018	0.664
TA 1504	19.245	8.391	1.398
NEE 1109	2.042	1.208	1.217
NSR 2512	0.485	0.319	0.540
NT 0905	16.755	16.351	3.323
NT 2510	1.192	0.956	0.891

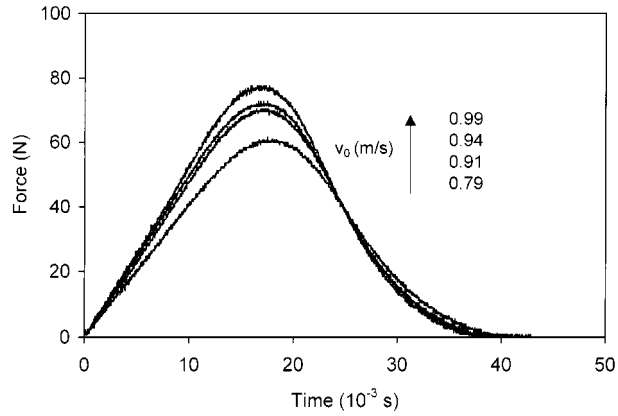

Figure 5 Typical force/time curves from flexed plate rebound tests (NEE 1109 foam).

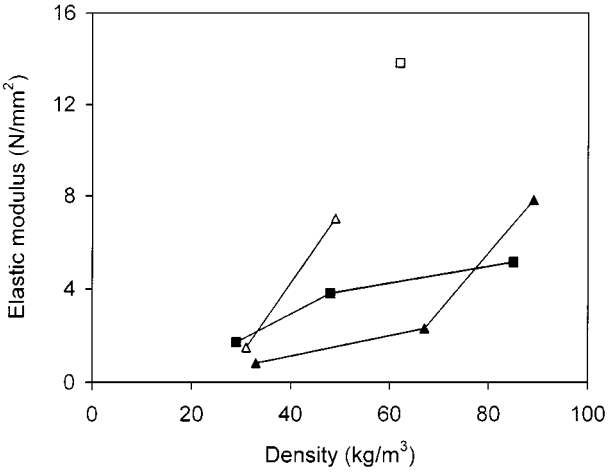

Figure 6 Average values of $E_{F\,\max}$ and E_{tc} versus foam density. Symbols as in Fig. 2.

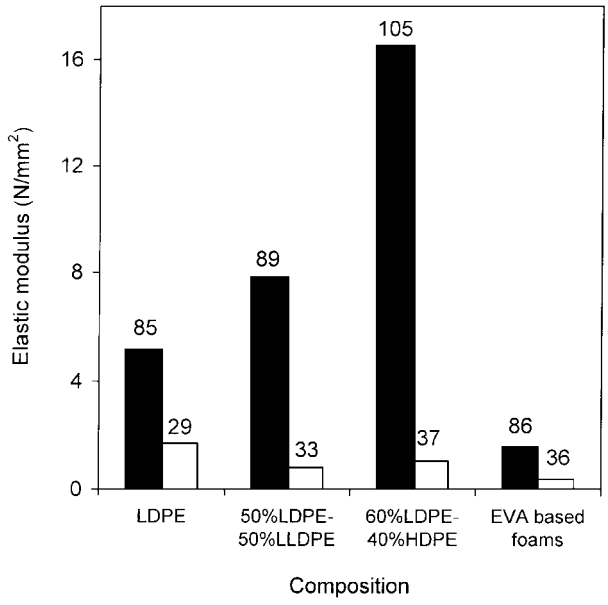

Figure 7 Influence of chemical composition on the elastic modulus obtained from flexed plate rebound tests.

to its high chain packaging degree, whereas the EVA based foam shows the lowest one because of its elastomeric character.

It must be also noted that the differences found between the values of the elastic modulus obtained from $F_{\max}$ and from t_c are considerably larger, 50% in some cases (e.g., TA 1504). These differences could be explained by focusing on the applied theory, which establishes that the materials must be fully linear-elastic in all the range of load applied, and that the specimen must be flexed during the load application. However, during the rebound tests, the studied foams showed that some of strain was caused by the dart indentation in addition to the flexion, which is due to their softness. This contribution is not taking into account in the simple model for flexed plates. Moreover, as is well known, the polymeric materials also can suffer plastic strain at low stress levels, and therefore the quasi-static model must only be applied as a first approximation to the elastic modulus determination of foams by means of this kind of rebound test. These circumstances make us consider that, although the main tendencies of the E values seems to be logical with regard to the foam density and chemical composition, one should not take the obtained values as material properties at relatively high strain rates.

5.3. Elastic modulus from indentation tests

The rigidity of the striker (k_1) was equal to 1.38×10^{-6} mm^2/N, considering $\nu_1 = 0.3$ and $E_1 = 2.1 \times 10^5$ N/mm^2. Then to obtain the rigidity of each foam (k_2), and so the elastic modulus (E_{ind}), the $F_{\max}$, and t_c values were taken from the experimental force/time curves in the indentation test. Fitting linearly the $F_{\max}$ and t_c values versus $v_0^{6/5}$ and $v_0^{-1/5}$ respectively (Equation 28 and Equation 30), the values of k_2 from both slopes were obtained, as shown in Fig. 8.

The obtained values of E_{ind} are shown in Table III, and, as it happened with flexed plate geometry, the elastic modulus increases with the foam density (Fig. 9).

It is important to note here that the E_{ind} values were found to be similar to those obtained by pure compression tests at low strain rates [16], but considerably lower than those obtained from the previous rebound tests with flexed plate geometry, which resulted in overestimated values due to the material compaction caused by the dart indentation effects.

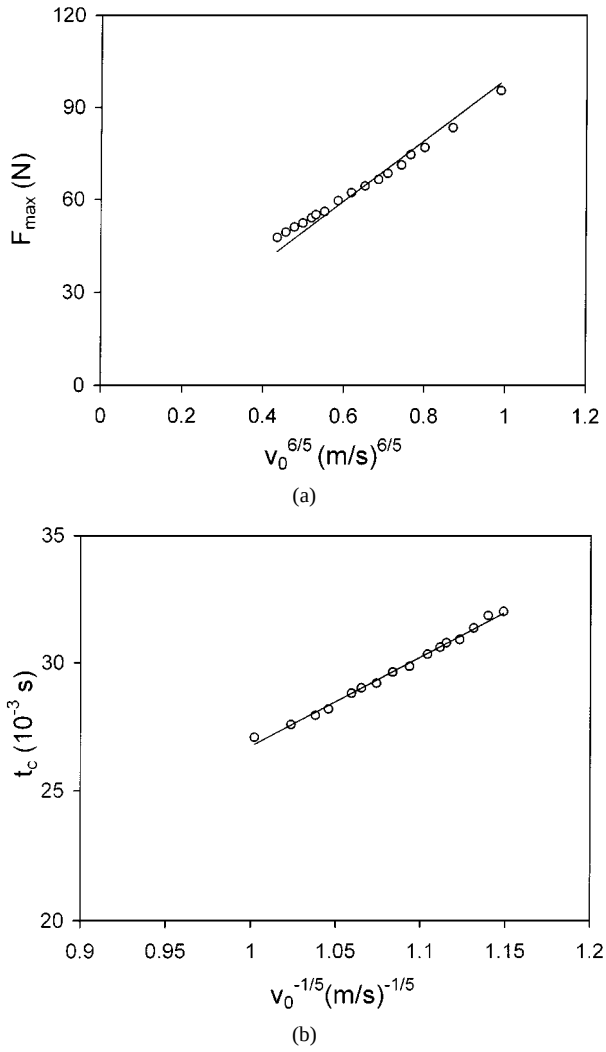

Figure 8 (a) Linear fitting of $F_{\max}$ and (b) t_c for NT 2510 sample.

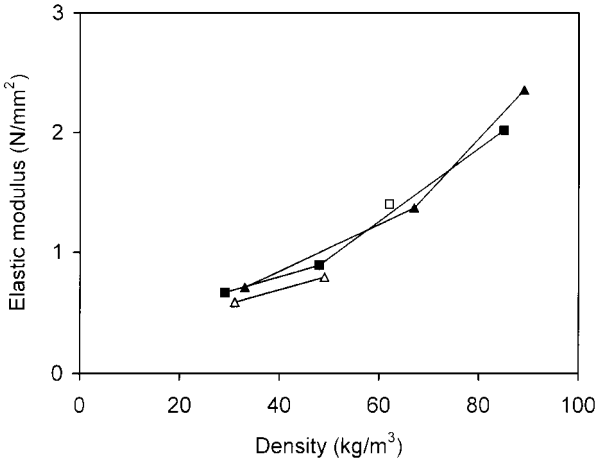

Figure 9 Influence of the foam density on the elastic modulus obtained from indentation tests. Symbols as in Fig. 2.

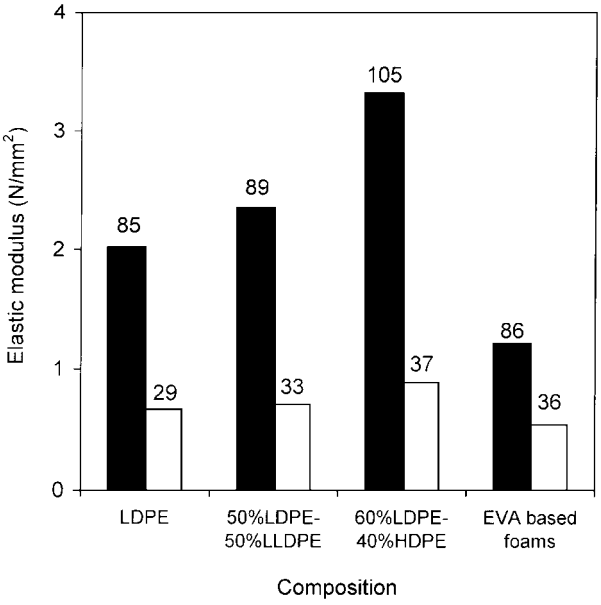

Figure 10 Influence of chemical composition on the elastic modulus obtained from indentation tests.

Here, the foaming process seems not to affect significantly the E_{ind} value because, using pure indentation geometry, the sample is only subjected to compression stresses. Therefore, the different cell morphology and molecular orientation generated in the foaming processes does not influence significantly the sample rigidity, unlike flexed plate geometry where the higher cell elongation of the T samples contributed to the increase in sample rigidity resulting from the presence of tensile stresses. The influence of the chemical composition of the foams on the E_{ind} values showed the following trend (Fig. 10): LDPE/HDPE > LDPE/LLDPE > LDPE > EVA.

6. Conclusions

A series of polyolefinic foams, with different chemical composition, density, and foaming processes, has been characterized mechanically at relatively high speed by means of instrumented falling dart tests. The foam toughness and strength measured from high-energy tests increased as the foam density did. The foaming process did not affect the foam toughness, but did affect the foam strength. The foams containing HDPE showed the highest strength and the lowest toughness, whereas the EVA-based foam showed the opposite trend.

The elastic modulus of the foams was measured by two kinds of low-energy tests. Because of their softness, the studied foams suffered important indentation effects when they were subjected to rebound tests with flexed plate geometry. These indentation effects provoked the foam compaction in addition to the sample flexion, resulting in higher values of the elastic modulus than those obtained by indentation tests and those expected if there were just flexion. This contribution is not taken into account in the quasi-static model. Thus it seems more accurate to use indentation low-energy impact tests to determine the elastic modulus of these materials at relatively high speeds.

Finally, the foaming process seemed not to affect the elastic modulus when measured from indentation tests, and the influence of the foam chemical composition on this property was found to be similar to that of the foam strength.

References

1. ISO/DIS 6603-1, "Plastics-Determination of puncture impact behavior of rigid plastics," International organization for standarization (1997).
2. J. G. WILLIAMS, in "Fracture Mechanics of Polymers" (Ellis Horwood Ltd., London, 1984) p. 41.
3. A. J. KINLOCH, G. A. KODOKIAN and M. B. JAMARANI, *J. Mater. Sci.* **22** (1987) 4111.
4. N. J. MILLS and A. M. H. HWANG, *Cell. Polym.* **9** (1989) 259.
5. P. LOVERIDGE and N. J. MILLS, *ibid.* **12** (1992) 393.
6. T. CASIRAGHI, G. CASTIGLIONI and T. RONCHETTI, *J. Mater. Sci.* **23** (1988) 459.
7. A. B. MARTÍNEZ, J. ARNAU, O. SANTANA and A. GORDILLO, *Inf. Tec.* **5** (1994) 19.
8. L. B. GRESZCUK, in "Impact Dynamics," edited by L. B. Greszczuk, J. A. Zukas, T. Nicholas, H. F. Swift and D. R. Curran (John Wiley & Sons, New York, 1982) p. 55.
9. L. RAYLEIGH, *Phil. Mag.* **11** (1906) 283.
10. H. HERTZ and J. REINE, *Ang. Math.* **92** (1881) 156.
11. S. P. TIMOSHENKO, in "Theory of elasticity" (McGraw-Hill, New York, 1934).
12. M. A. RODRÍGUEZ-PÉREZ, O. ALONSO, J. SOUTO and J. A. DE SAJA, *Polym. Test.* **16** (1997) 287.
13. S. P. TIMOSHENKO and S. WOINOWSKY-KRIEGER, in "Theory of plates and shells" (McGraw-Hill, New York, 1984) p. 71.
14. L. J. GIBSON and M. F. ASHBY, in "Cellular Solids: Structure and Properties" (Pergamon Press, Oxford, 1988) p. 43.
15. P. R. HORNSBY, in "Two-Phase Polymer Systems," edited by L. A. Utracki (Carl Hanser Verlag, Munich, 1991) p. 93.
16. M. A. RODRÍGUEZ-PÉREZ, J. I. VELASCO, D. ARENCÓN, O. ALMANZA and J. A. DE SAJA, *J. Appl. Polym. Sci.* (submitted, 1998).

Received 12 August
and accepted 26 August 1998